# REPORT No. 635

## THEORETICAL STABILITY AND CONTROL CHARACTERISTICS OF WINGS WITH VARIOUS AMOUNTS OF TAPER AND TWIST

By Henry A. Pearson and Robert T. Jones

### SUMMARY

*Stability derivatives have been computed for twisted wings of different plan forms that include variations in both the wing taper and the aspect ratio. Taper ratios of 1.0, 0.50, and 0.25 are considered for each of three aspect ratios: 6, 10, and 16. The specific derivatives for which results are given are the rolling-moment and the yawing-moment derivatives with respect to (a) rolling velocity, (b) yawing velocity, and (c) angle of sideslip. These results are given in such a form that the effect of any initial symmetrical wing twist (such as may be produced by flaps) on the derivatives may easily be taken into account.*

*In addition to the stability derivatives, results are included for determining the theoretical rolling moment due to aileron deflection and a series of influence lines is given by which the loading across the span may be determined for any angle-of-attack distribution that may occur on the wing plan forms considered. The report also includes incidental references to the application of the results.*

### INTRODUCTION

Although a formal theory for the dynamics of airplane motions has been available for many years, airplane designers have not been in a position to utilize this theory to its fullest advantage on account of lack of knowledge of the basic physical quantities involved. It is true that the physical quantities, or stability derivatives, have been determined by test or calculation in a number of instances, but there exists no systematic series or correlation of tests sufficient to guide the designer in the prediction of these factors.

As is well known, the calculations involved in aerodynamic wing theory have been developed and refined to such an extent that it is possible to predict quite accurately the air moments and forces on the isolated wing at a fixed speed and incidence. Since several of the airplane lateral-stability derivatives depend almost entirely on the aerodynamic characteristics of the wing and since it would be desirable in any case to know the separate effects of variation of wing form on stability, it was thought worth while to extend the calculations to the determination of the moments developed by the wings when the airplane is disturbed from steady flight. This report gives theoretical stability derivatives for a variety of wing shapes including nine different plan forms and covering, in most cases, an arbitrary distribution of twist.

Past work on the stability characteristics of wings has, except in isolated cases, been confined to analysis by the "strip method," wherein the effects of aerodynamic induction were neglected. The main effects of the induction are included in the present computations, although the secondary influence of distortion or curvature of the wake is neglected.

### DEFINITIONS

The axes used in specifying moments, angular velocities, etc., are fixed in the wing and therefore move relatively to the air and to the earth. The $X$ axis passes through the wing aerodynamic center in the plane of symmetry and is so chosen as to point directly into the line of the relative wind when the wing is moving steadily. Otherwise the axes form an orthogonal system as shown in the back cover of the report.

The derivatives that may be obtained enable an estimate to be made of the variation of both rolling moment and yawing moment with (1) rolling velocity, (2) yawing velocity, and (3) sideslip angle. These factors, designated by $C_{l_p}$, $C_{n_r}$, etc., are to be used in the following general formulas to determine the wing rolling and yawing moment in combined rolling, yawing, and sideslipping motion:

$$\frac{L}{qSb}=C_{l_p}\left(\frac{pb}{2V}\right)+C_{l_r}\left(\frac{rb}{2V}\right)+C_{l_\beta}\beta \qquad (1)$$

$$\frac{N}{qSb}=C_{n_p}\left(\frac{pb}{2V}\right)+C_{n_r}\left(\frac{rb}{2V}\right)+C_{n_\beta}\beta \qquad (2)$$

Subscripts $p$ and $r$ are used to designate the partial derivatives of the well-known wing rolling-moment and yawing-moment coefficients, $C_l$ and $C_n$, with respect to instantaneous rolling and yawing angular velocities (expressed as helix angles) and $\beta$ is used to designate the partial derivatives of these coefficients with respect to instantaneous sideslip angles. In this manner the notation is considerably shortened from the usual more cumbersome expressions $\partial C_l/\partial\left(\frac{pb}{2V}\right)$, $\partial C_n/\partial\left(\frac{rb}{2V}\right)$, etc. Expressing the rolling and yawing moments as the sums

of partial linear factors is considered valid for motions that are slow relative to the flight speed $V$ and for small displacements, such as occur in ordinary unstalled maneuvers and such as are considered in the study of stability.

$\alpha$, angle between the zero-lift direction of the wing section and the air velocity at infinity, radians.

$\theta$, parameter defining spanwise position, $y=-\frac{b}{2}\cos\theta$ $\left(\text{when } \theta=0,\ y=-\frac{b}{2};\ \theta=\pi,\ y=\frac{b}{2}\right)$.

$C_0$, $C_2$, $C_4$, coefficients of cosine series expressing wing plan form.

$C_l$, rolling-moment coefficient.

$C_n$, yawing-moment coefficient.

$p$, angular velocity in roll, radians per sec.

$r$, angular velocity in yaw, radians per sec.

$V$, flight velocity of wing along $X$, f. p. s.

$\beta$, angle of sideslip, radians.

$\delta$, aileron deflection, radians.

$C_{l_p}$, rate of change of rolling-moment coefficient $C_l$ with the helix angle $pb/2V$.

$C_{n_p}$, rate of change of yawing-moment coefficient $C_n$ with the helix angle $pb/2V$.

$C_{l_r}$, rate of change of rolling-moment coefficient $C_l$ with the helix angle $rb/2V$.

$C_{n_r}$, rate of change of yawing-moment coefficient $C_n$ with the helix angle $rb/2V$.

$C_{l_\beta}$, rate of change of rolling-moment coefficient $C_l$ with sideslip angle $\beta$.

$C_{n_\beta}$, rate of change of yawing-moment coefficient $C_n$ with sideslip angle $\beta$.

$C_{l_\delta}$, rate of change of rolling-moment coefficient $C_l$ with aileron angle $\delta$.

$C_{n_\delta}$, rate of change of yawing-moment coefficient $C_n$ with aileron angle $\delta$.

$L$, total wing rolling moment, ft.-lb.

$N$, total wing yawing moment, ft.-lb.

$q$, dynamic pressure, lb. per sq. ft.

$S$, wing area, sq. ft.

$c$, chord length at any section, ft.

$c_s$, chord length at plane of symmetry, ft.

$m_0$, section slope of the lift curve, per radian.

$b$, wing span, ft.

$A$, wing aspect ratio, $b^2/S$.

$A_n$, $B_n$, $C_{2n}$, coefficients of Fourier series. (See reference 2.)

$c_l$, section lift coefficient, section lift/$qcdy$.

$C_L$, wing lift coefficient, wing lift/$qS$.

$c_{d_0}$, section profile-drag coefficient.

$c_{d_i}$, section induced-drag coefficient.

$C_{D_0}$, wing profile-drag coefficient.

$\lambda$, taper ratio: i. e., ratio of the fictitious tip chord, obtained by extending the wing leading and trailing edges to the tip, to the root chord.

$\Gamma$, dihedral angle, radians.

## CONDITIONS RELATING TO THE COMPUTATIONS

### PLAN FORMS

The particular chord distributions for which the computations were made are illustrated in figure 1. Table I gives the coefficients of the cosine series used to express these chord distributions in terms of $\theta$. Although the quarter-chord line is shown to be straight, it is permissible to apply the results to wings with similar chord distributions but with the different plan forms that

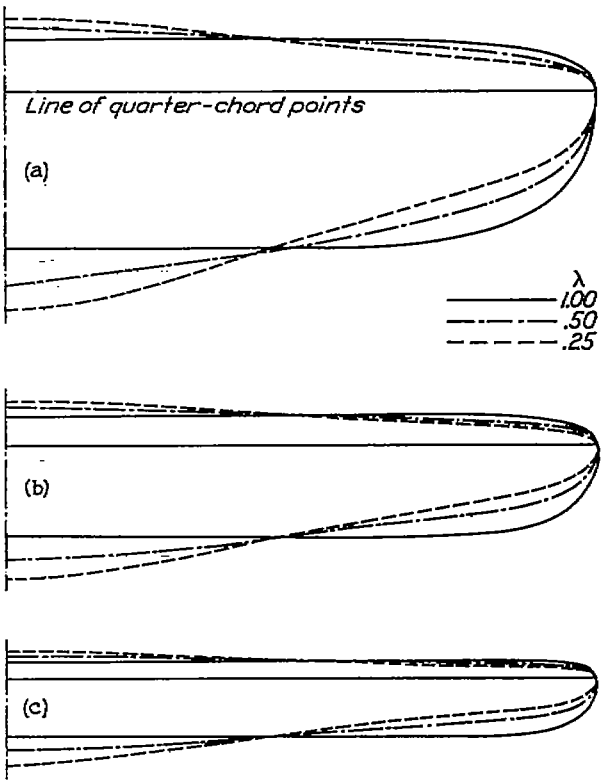


(a) $A=6$.
(b) $A=10$.
(c) $A=16$.

FIGURE 1.—Wing plan forms considered.

may be obtained by small alterations of the shape of the quarter-chord line. The computations were made for three aspect ratios, 6, 10, and 16, and for three taper ratios, 1.00, 0.50, and 0.25. The wing plan forms used only approximate those of linearly tapered wings with rounded tips.

### LIFT DISTRIBUTIONS

Rolling, yawing, and sideslipping motions introduce varying resolutions of the relative-wind velocity over the wing. It is evident that these variations can, to a certain extent, be replaced by a fictitious warp or twist of the wing in straight flight. The procedure followed here is to calculate the spanwise lift and drag distributions for the fictitious twist (i. e., that replacing the effect of motion) in the ordinary way, but to incline the

# E R R A T A

NACA Report No. 635

## THEORETICAL STABILITY AND CONTROL CHARACTERISTICS OF WINGS WITH VARIOUS AMOUNTS OF TAPER AND TWIST

By Henry A. Pearson and Robert T. Jones

1938

The values of $C_{n_r}/\alpha^2$ given in figures 12 and 13 have been found to be in error because of the omission of a term in the expansion of the formula for the yawing derivative due to yawing. The correct values for these figures, which have been supplied by LMAL, may be obtained from the following table:

VALUES OF $C_{n_r}/\alpha^2$

| A \ Extent of flap from wing center | 0.25 | 0.50 | 0.75 | 1.00 |
|---|---|---|---|---|
| $\lambda = 0.25$ | | | | |
| 6 | [a]0.006 | 0.058 | [a]0.175 | 0.290 |
| 10 | [a].008 | .052 | [a].135 | .220 |
| 16 | [a].005 | .039 | [a].098 | .147 |
| $\lambda = 0.50$ | | | | |
| 6 | [a]0.002 | 0.060 | [a]0.208 | 0.364 |
| 10 | [a].004 | .050 | [a].165 | .284 |
| 16 | [a].003 | .039 | [a].120 | .211 |
| $\lambda = 1.00$ | | | | |
| 6 | [a]−0.001 | 0.059 | [a]0.240 | 0.450 |
| 10 | [a].001 | .044 | [a].182 | .365 |
| 16 | [a]−.001 | .035 | [a].149 | .297 |
| Elliptical wing | | | | |
| 10 | 0.006 | 0.060 | 0.142 | 0.242 |

[a]Obtained from faired curves.

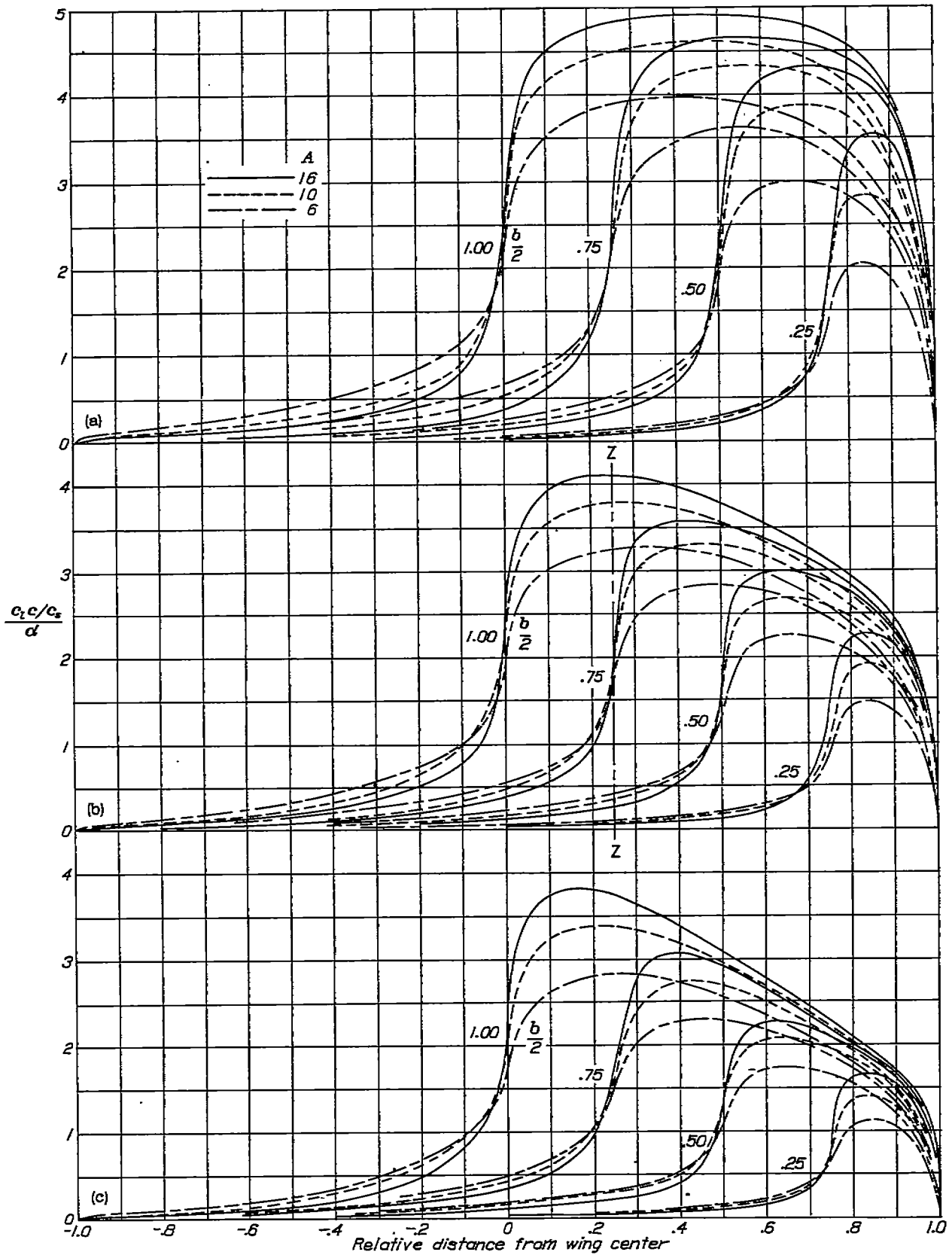


(a) λ=1.00. (b) λ=0.50. (c) λ=0.25.

FIGURE 2.—Load distribution due to unit angles of attack extending inward from the tip.

lift and drag components so as to maintain them along the perpendicular and the parallel to the actual local relative-wind velocity. A further refinement of the theory would involve the influence of the curvature of the wing wake. Since the helix angles involved in the motions are small ($pb/2V<0.1$ and $rb/2V<0.1$) and since that region of the wake nearest the wing is of predominant influence, this correction may be neglected.

Inasmuch as the various stability derivatives thus depend upon a summation of appropriate components of the lift and the drag loading along the span, it was necessary to determine these distributions for each of the wings with several different angle-of-attack distributions. For this purpose the Lotz method of calculation (references 1 and 2) was used. In order to keep the computations from becoming too lengthy, the chord-distribution function that occurs in this method was expressed by, at most, three terms of a cosine series (as in table I). Although this expression caused the chord distributions of the actual wings (fig. 1) to differ slightly from those for linearly tapered wings with rounded tips, such a procedure was justified because these slight departures in plan form had only a small effect on the characteristics but permitted a large saving in the computations required. Thus only the terms near the diagonal running through equations (19) of reference 2 entered into the computations. As the various derivatives for the elliptical wing could be obtained relatively easily, they were sometimes computed in order to determine the shape of the various derivative curves; it was therefore possible to use fewer points in fairing similar curves for the tapered wings.

The wing theory was applied in a special way so as to obtain results applicable to any arbitrary twist of the wings. The theoretical span loading being a linear function of the angle-of-attack distribution, the loading due to arbitrary twist can be built up, as will be indicated later, from certain elementary loadings by superposition. The elementary loadings considered were those caused by simple unit jumps of angle of attack occurring at different points of the span.

For each of the nine tapered wings, the first 20 Fourier coefficients determining the load distributions were computed (10 odd and 10 even) for the cases of unit angles of attack extending inward from the wing tip and covering various amounts of the semispan. The rest of the wing was in each case assumed to be at zero angle of attack. The portions thus covered were 0.25, 0.50, 0.75, and 1.00 of the semispan.

In spite of the great number of harmonic terms retained, the conditions near the points of discontinuity in the angle of attack required special treatment. The problem of these end conditions has been solved by Betz and Petersohn (reference 3) and their results were utilized in fairing the load curves through this region. Figure 2 shows the elementary loadings that were calculated, including the modified fairing. The results pertain specifically to the chord distributions illustrated in figure 1 but interpolation might be made for intermediate plan forms.

It is evident that any angle-of-attack distribution, symmetrical or unsymmetrical, may be built up of elemental steps of the type used in deriving figure 2. Figure 3 illustrates the procedure of finding the resultant load distribution. Thus, the loading contributed by element 10 of figure 3 (a) is obtained by deducting the load curve due to an increment of angle of attack extending between B and C from that due to an increment extending between A and C. Although this process could be continued until the load distribution was completely determined, the same results can be more easily obtained from influence lines, which give the load at a particular spanwise station due to the effect of unit angle-of-attack changes extending inward various

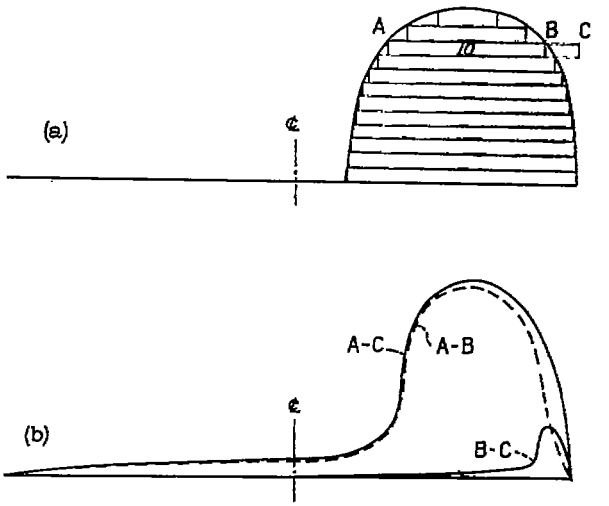


(a) Angle-of-attack distribution.
(b) Load distribution for element (10).

FIGURE 3.—Load components for an element.

amounts from the right wing tip. Such influence lines are given in figures 4, 5, and 6 for eight evenly spaced points across the wing semispan. Each line was obtained by cross-plotting the values of $\frac{c_l c/c_a}{\alpha}$ at the intersections of the loading curves of figure 2 with vertical lines drawn at the particular stations. (For example, the points of intersection of line Z—Z, fig. 2 (b), with the various curves represent the load induced at the 0.25-semispan point by uniform angle-of-attack increments that extend in varying amounts from the wing tip. These intersections identify the corresponding curves of figs. 4 to 6.)

In order to illustrate the use of the influence lines in determining the lift distribution as well as to show the degree of accuracy with which they may be used, the influence lines will be applied to predict the loading for a tapered wing ($\lambda=0.25$, $A=6$) corresponding to the angle-of-attack distribution shown in figure 7 (a). The particular angle-of-attack distribution used is defined by the equation

$$\alpha=\left(\frac{c_s}{c}+\frac{3c_s m_0}{4b\sin\theta}\right)\sin 3\theta \qquad (3)$$

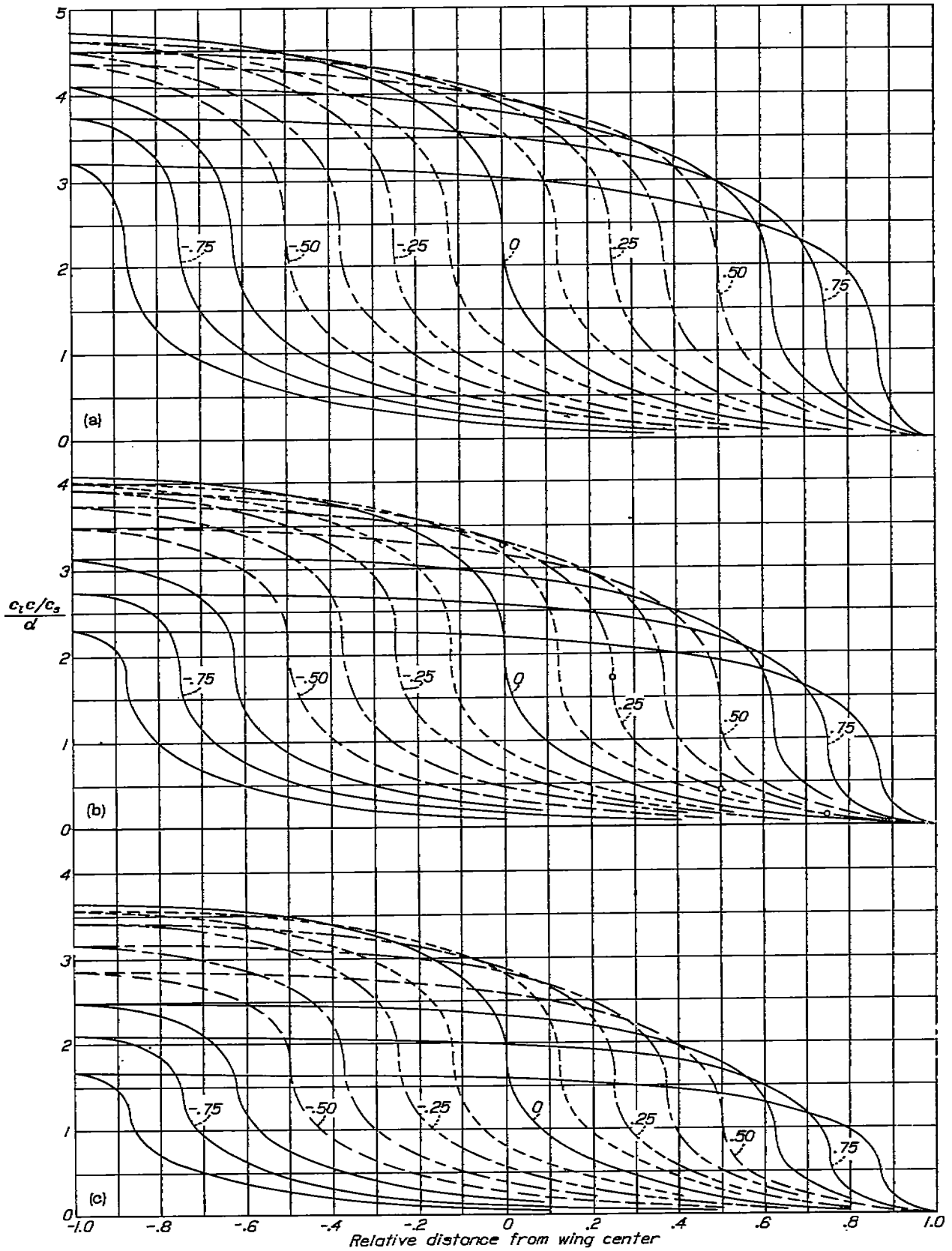


(a) $\lambda$=1.00. (b) $\lambda$=0.50. (c) $\lambda$=0.25.

FIGURE 4.—Influence lines for determining the load distribution. $A$=6. The number identifying a given line refers to the particular spanwise station at which the load is to be computed.

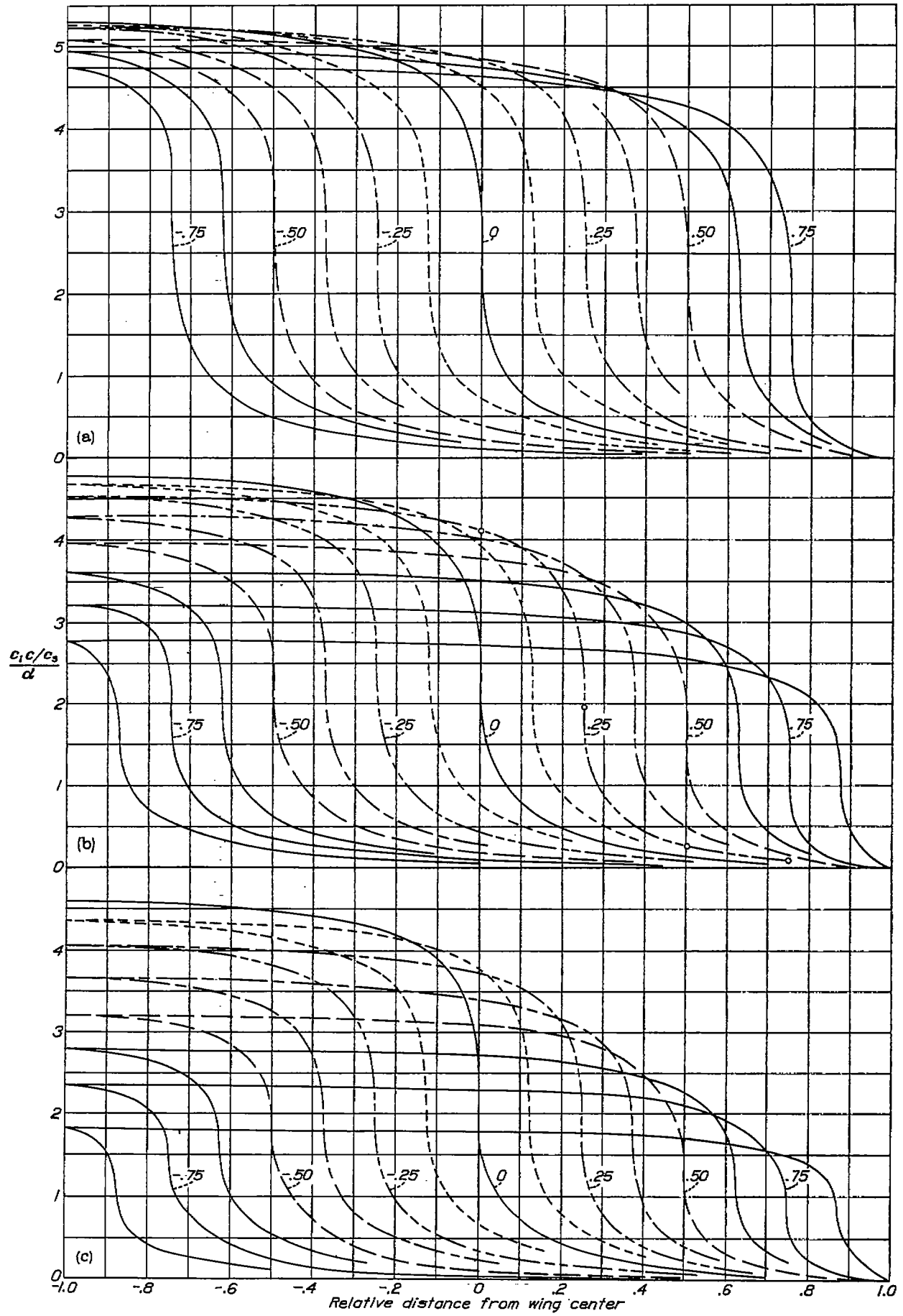


(a) $\lambda=1.00$ (b) $\lambda=0.50$. (c) $\lambda=0.25$.

FIGURE 5.—Influence lines for determining the load distribution. $A=10$. The number identifying a given line refers to the particular spanwise station at which the load is to be computed.

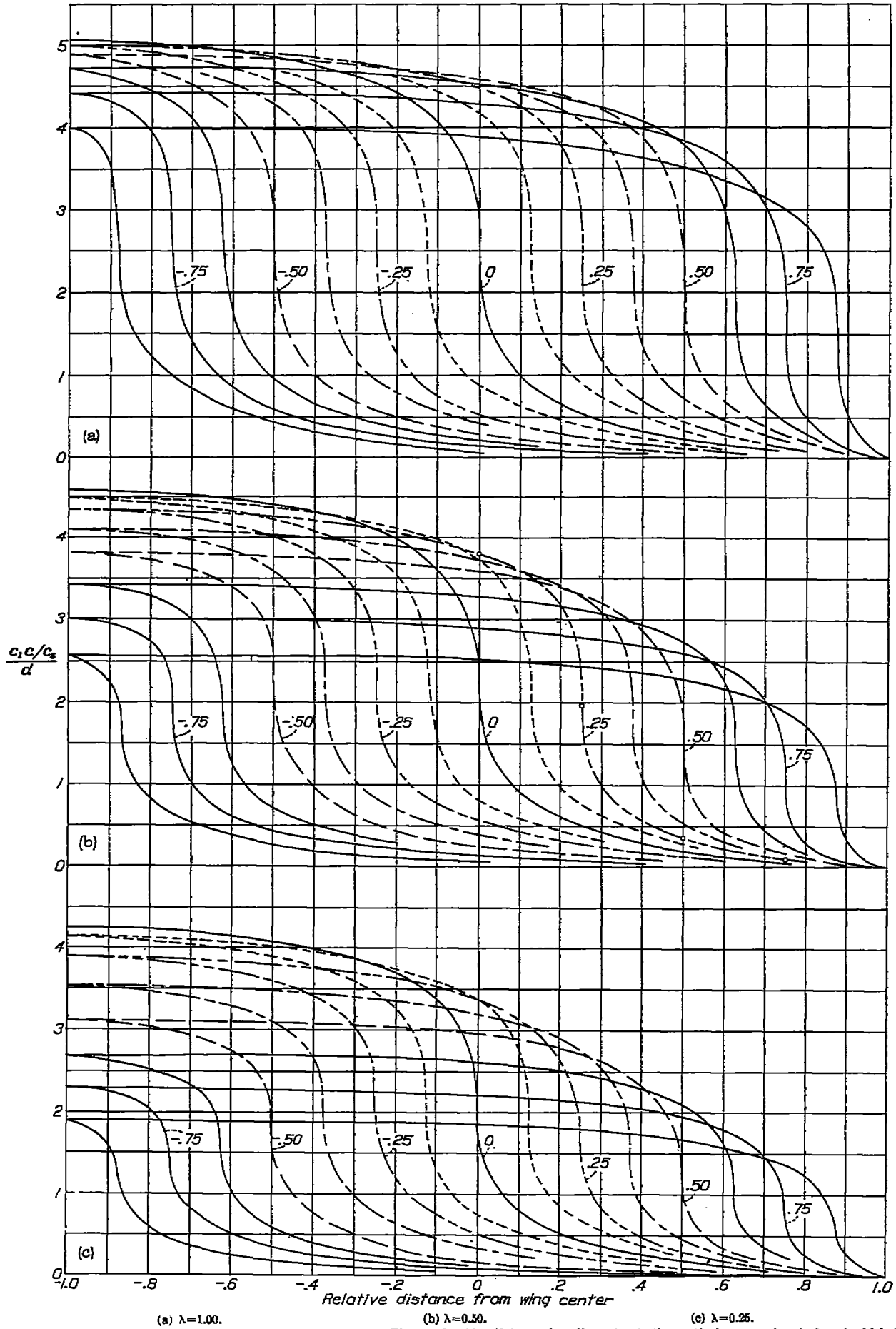


(a) λ=1.00. (b) λ=0.50. (c) λ=0.25.

FIGURE 6.—Influence lines for determining the load distribution. $A=16$. The number identifying a given line refers to the particular spanwise station at which the load is to be computed.

This particular distribution is employed because it is possible thereby to compute exactly the corresponding theoretical distribution as a check, without the usual approximations of a Fourier series. The following procedure illustrates the use of the influence lines to determine the lift at the 0.75-semispan point due to this distribution of twist: (1) The influence curve labeled 0.75 in figure 4 (c) is reproduced beneath the angle distribution to the same spanwise scale; (2) a base line with a range from $\alpha_{max-}$ to $\alpha_{max+}$ is laid out as in figure 7 (c) with the origin of the ordinates at $\alpha$ equal to zero; (3) the effect of any length of elemental angle-of-attack change, $d\alpha$, in figure 7 (a) is found by projecting the length of the element onto figure 7 (b) and plotting the increments ($\Delta_1$) and ($\Delta_2+\Delta_2'$) at the angles of attack for which these elements are drawn, as in figure 7 (c). Because a negative angle would induce a negative load at the point in question, $\Delta_1$ is plotted as a negative value. This process is continued from $\alpha_{max-}$ to $\alpha_{max+}$ and the resulting curve (fig. 7 (c)) is integrated to obtain the total effect at 0.75, which is then plotted in figure 7 (d). The load distribution over the entire span is obtained by repeating the same procedure for a number of points along the span.

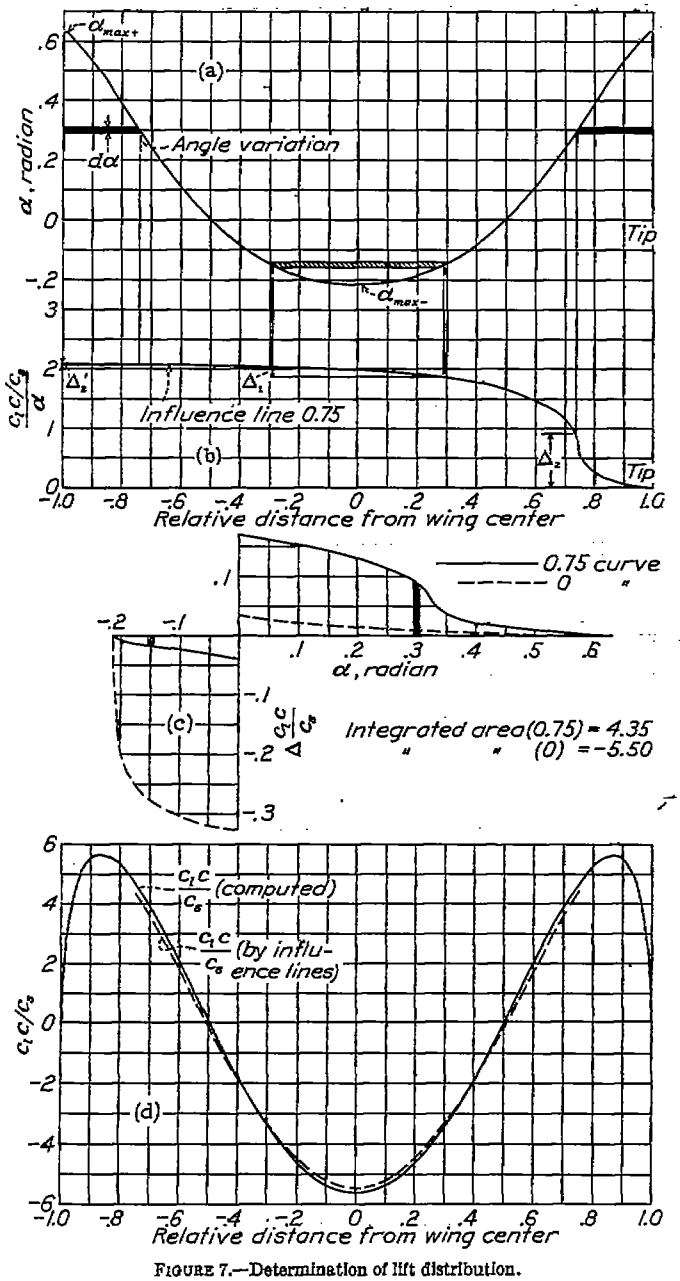


FIGURE 7.—Determination of lift distribution.

With the lift loading thus determined, the induced-drag distribution may be found by a simple operation, namely

$$c_{d_i}=c_l\left(\alpha-\frac{c_l}{m_0}\right) \tag{4}$$

Figure 7 (d) gives the comparison of the load-distribution curve obtained from the influence lines with that computed directly by the wing theory using equation (3). Although the agreement is not precise, it must be remembered that the solid curve represents a case where no series approximation was necessary; hence it may be concluded that the influence-line method of determining the lift distribution is as accurate as any other for practical purposes.

Aside from other possible applications, the load distribution may be used to determine the stability derivatives for certain cases not specifically covered by the calculations. In the subsequent charts, it is sometimes necessary to stipulate either that the initial angle-of-attack distribution be symmetrical about the wing center line or that the dihedral angle be constant along the span. With a knowledge of the complete load distribution, however, values of the derivatives or their respective moments might be found for particular cases where the charts do not apply.

## STABILITY DERIVATIVES

Although it is possible, in the general case, to obtain the stability derivatives from the lift distribution, such a procedure will not usually be necessary because the charts to be presented cover all cases likely to be of interest. The results are presented in such a form that the effect of flaps on the derivatives may easily be determined.

### ROLLING MOMENT DUE TO ROLLING

The first derivative considered is the rolling moment due to rolling. In unstalled flight, when the wing rolls about the longitudinal wind axis, a damping or restoring moment is set up. This moment $L_{rolling}$ varies directly with the angular velocity $p$ and is defined by the equation

$$L_{rolling}=C_{l_p}\frac{pb}{2V}qSb \tag{5}$$

where the product $C_{l_p}\frac{pb}{2V}$ is simply a rolling-moment coefficient that varies linearly with the angular velocity.

The computed variation of the derivative $C_{l_p}$ with aspect ratio and taper is given in figure 8. In the usual lift range below the stall, this derivative may be considered to be independent of either initial wing twist or angle of attack and of the wing dihedral. In conventional cases, practically the entire damping moment for the airplane may be attributed to the wings. It can be seen that the moment contributed by a tail surface, geometrically similar to the wing but with only one-

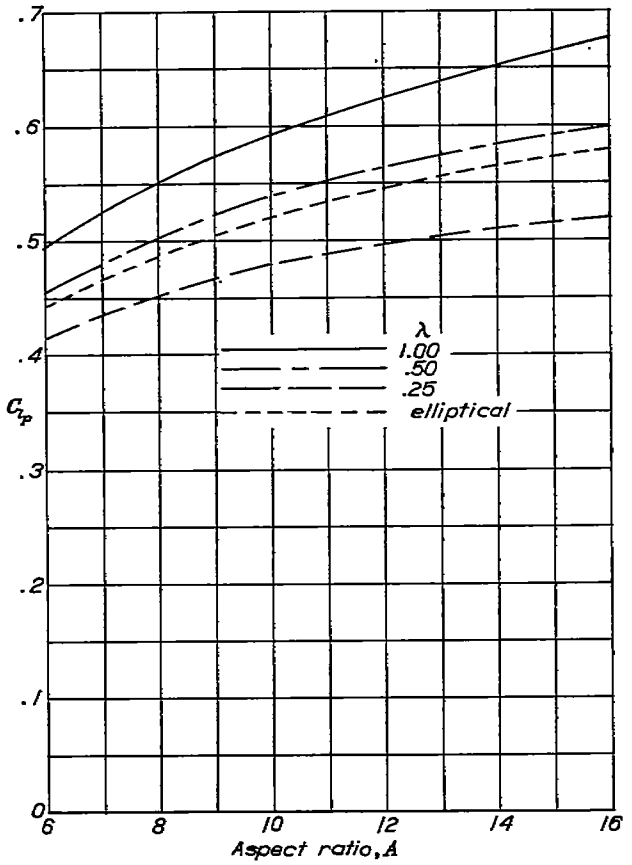


FIGURE 8.—Rolling derivative due to rolling. $L_{rolling}=C_{l_p}\frac{pb}{2V}qSb$

fourth the span, would be $\frac{1}{256}$ of that contributed by the wing, inasmuch as $L_{rolling}$ for a given angular velocity varies as the fourth power of a linear dimension.

Reducing the aspect ratio or increasing the taper tends to reduce the derivative $C_{l_p}$, as may be seen from the curves given in figure 8. Comparison of the present values of $C_{l_p}$ with similarly derived values given in reference 4 indicates that the effect of rounding the wing tips is to reduce the theoretical restoring moment by about 6 percent for wings of aspect ratio 6.

### YAWING MOMENT DUE TO ROLLING

During a rolling motion, the wing experiences a linear antisymmetrical change in angle of attack along the span and, as a result, antisymmetrical loadings are added to those that originally were on the wing. The resulting yawing moment is due to components of the lift as well as to the drag along the span, the lift components being the more important. With the specified system of axes, positive rolling produces a negative yawing moment or, for any case, with positive lift coefficients the falling wing tends to advance owing to the predominating influence of the lift vectors.

The yawing moment due to rolling, unlike the rolling moment due to rolling, depends upon both the initial wing twist and the angle of attack. For untwisted wings, however, the yawing moment is zero at zero lift and increases linearly with the wing lift coefficient. For a twisted wing, the yawing moment due to rolling, although varying linearly with the over-all lift coefficient, is not necessarily zero when $C_L$ is zero but may have either a small positive or a small negative value depending upon the initial angle-of-attack distribution. Owing to this circumstance, it is most convenient to express the derivative $C_{n_p}$ as a ratio in terms of unit partial-span angle-of-attack changes.

Figure 9 shows the computed variation of the ratio $C_{n_p}/\alpha$ for unit symmetrical angle-of-attack changes that extend out from the wing center so as to cover various amounts of the wing span. Thus, if it is desired to determine $C_{n_p}$ for an untwisted rectangular wing of aspect ratio 6 at an angle of attack of 0.1 radian, the value 0.195 (for an angle of attack of 1 radian), read from the solid line of figure 9 (a) at the relative distance of 1.0, is multiplied by 0.1 to give a value of $C_{n_p}$ equal to 0.0195. If, now, a half-span flap of constant chord ratio were displaced an amount sufficient to cause an additional change in angle equal to 0.1 radian over the portion with flaps, the new value of $C_{n_p}$ would be

$$(0.1\times 0.195)+(0.1\times 0.134)=0.0329$$

This value of $C_{n_p}$ is then inserted into the equation

$$N_{rolling}=C_{n_p}\frac{pb}{2V}qSb \qquad (6)$$

to determine the yawing moment due to a rolling angular velocity.

Although the curves given in figure 9 can be directly used to determine the effect on $C_{n_p}$ of deflecting partial-span flaps of constant flap-chord ratio, they are also readily adapted to the determination of $C_{n_p}$ for a wing with any initial twist provided that the twist distribution is symmetrical about the wing center line. The process is illustrated in the following example where it is desired to find the value of $C_{n_p}$ for a rounded-tip rectangular wing of aspect ratio 6 with the symmetrical angle-of-attack distribution shown in figure 10 (a). The contribution of the element of angle of attack $d\alpha$, shown at the point $\alpha=0.15$ radian, to the total value of the wing $C_{n_p}$ is equivalent to that caused by a full-span elemental flap minus the contribution of the cross-hatched portions. The contribution of this element $d\alpha$ is denoted by $\left(\frac{C_{n_p}}{\alpha}\right)d\alpha$ and may be obtained

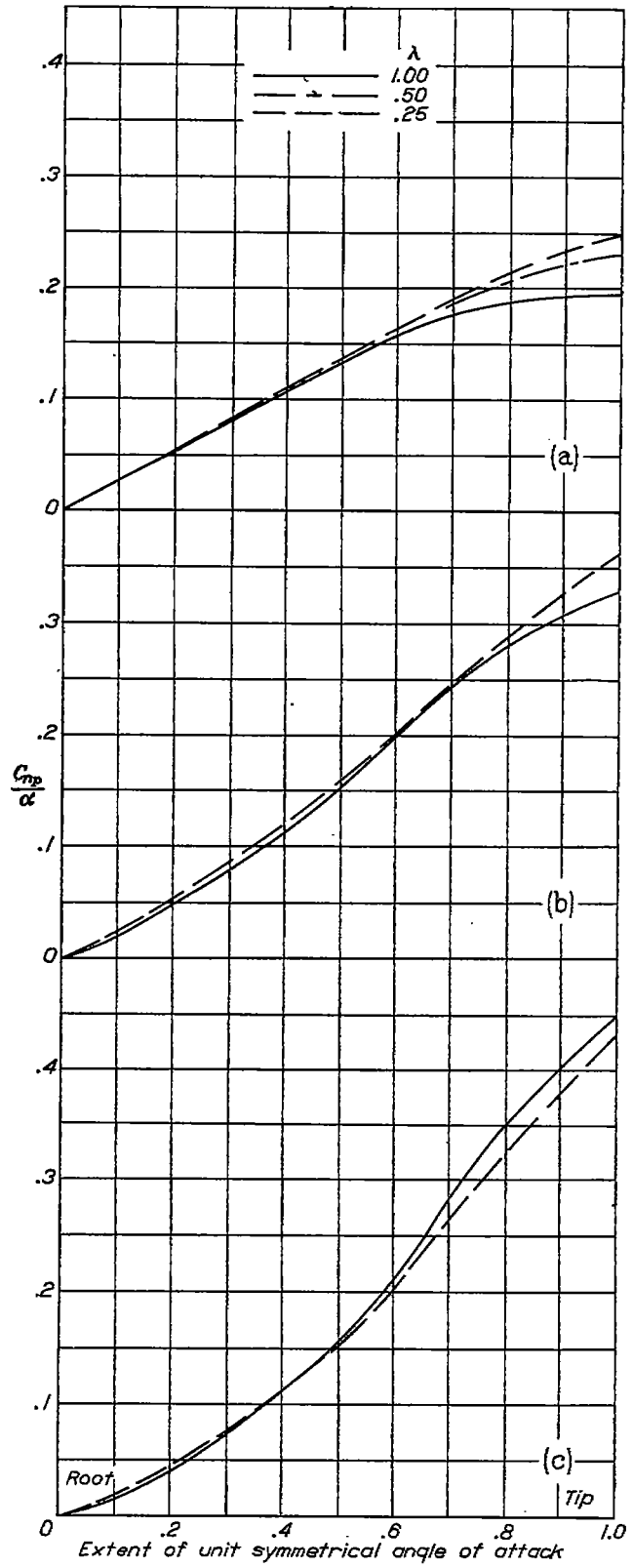


(a) $A=6$.
(b) $A=10$.
(c) $A=16$.

FIGURE 9.—Yawing derivative due to rolling. $N_{rolling}=C_{n_p}\frac{pb}{2V}qSb$

by projecting the various small flap portions onto the appropriate $C_{n_p}/\alpha$ curve (taken from fig. 9) as in figure 10 (b), and adding the increments $\Delta_1$ and $\Delta_2$. The sum of these increments is then plotted in figure 10 (c) at the value of $\alpha$ for which the element is drawn. The value of $C_{n_p}$ for the complete wing is obtained by performing the integration

$$C_{n_p}=\int_0^{\alpha_{max+}}\left(\frac{C_{n_p}}{\alpha}\right)d\alpha \qquad (7)$$

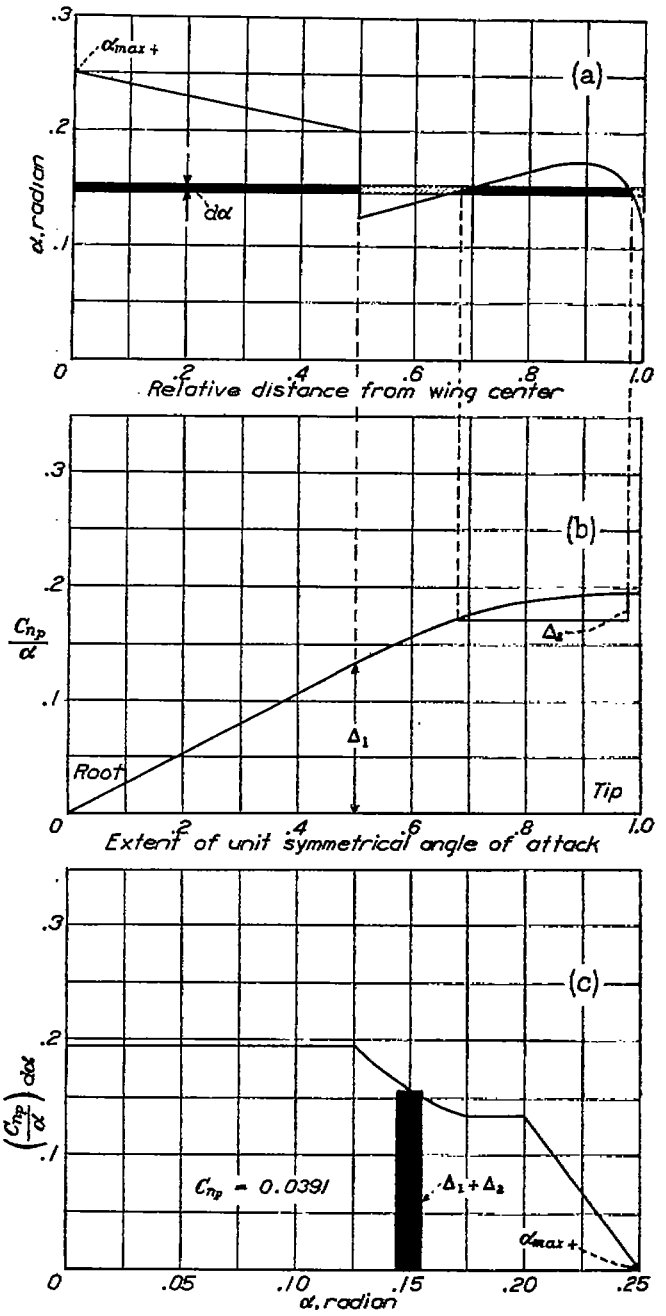


FIGURE 10.—Application of $C_{n_p}$ curves to an example.

These curves apply to wings with symmetrical twist and it is necessary to consider only half the wing, the factor 2 being included in the curves. The evaluation in the case of figure 10 (c) yields 0.0391.

The curves of figure 9 indicate that, for a given angle-of-attack distribution, there is relatively little change in the value of $C_{n_p}$ with the taper ratios investigated. Changes in taper ratio did, however, have an appreciable effect on the value of $C_{l_p}$ (fig. 8) with the result that the ratio of the yawing to the rolling moment in roll will, in general, increase with increase in taper.

Inasmuch as the inclination of the lift vectors at the outer portions of the span has such a predominating effect on the yawing moment, the most effective means of reducing $C_{n_p}$ for a given wing lift coefficient is to give the wings washout toward the tips.

The yawing moment due to rolling is, in conventional designs, largely due to the wings. The tail surfaces contribute very little to this moment both because of their short span and because of the small angles of attack relative to the wing.

### ROLLING MOMENT DUE TO YAWING

During a yawing motion, increments of velocity are added along the forward-moving half of the wing and similar increments are deducted along the rearward-moving half. The difference in velocity of the two halves causes a rolling moment which, for an untwisted wing, varies directly with the initial angle of attack as well as with the angular velocity. The velocity increments vary linearly with the distance from the wing center line and are small relative to the flight speed; it is therefore permissible to make certain mathematical approximations in deriving the necessary equations for the determination of the yawing derivatives. When these approximations are used and the velocity along the span is expressed as a variable, the new downwash equation becomes

$$w=\frac{V}{4\pi b}\int_0^{\pi}\frac{\left[\frac{d(c_l\alpha)}{d\theta}\left(1+\frac{rb}{2V}\cos\theta\right)-(c_l\alpha)\frac{rb}{2V}\sin\theta\right]}{\cos\theta-\cos\theta_0}d\theta \quad (8)$$

The system of simultaneous equations derived for the approximate solution of this integral equation is

$$\Sigma C_{2n}\cos 2n\theta\,\Sigma A_n\sin n\theta+\frac{c_l m_0}{4b}\Sigma nA_n\sin n\theta$$

$$+\frac{c_l m_0}{4b}\frac{rb}{4V}\Sigma(A_{n-1}-A_{n+1})\sin n\theta=\Sigma B_n\sin n\theta=\alpha\sin\theta \quad (9)$$

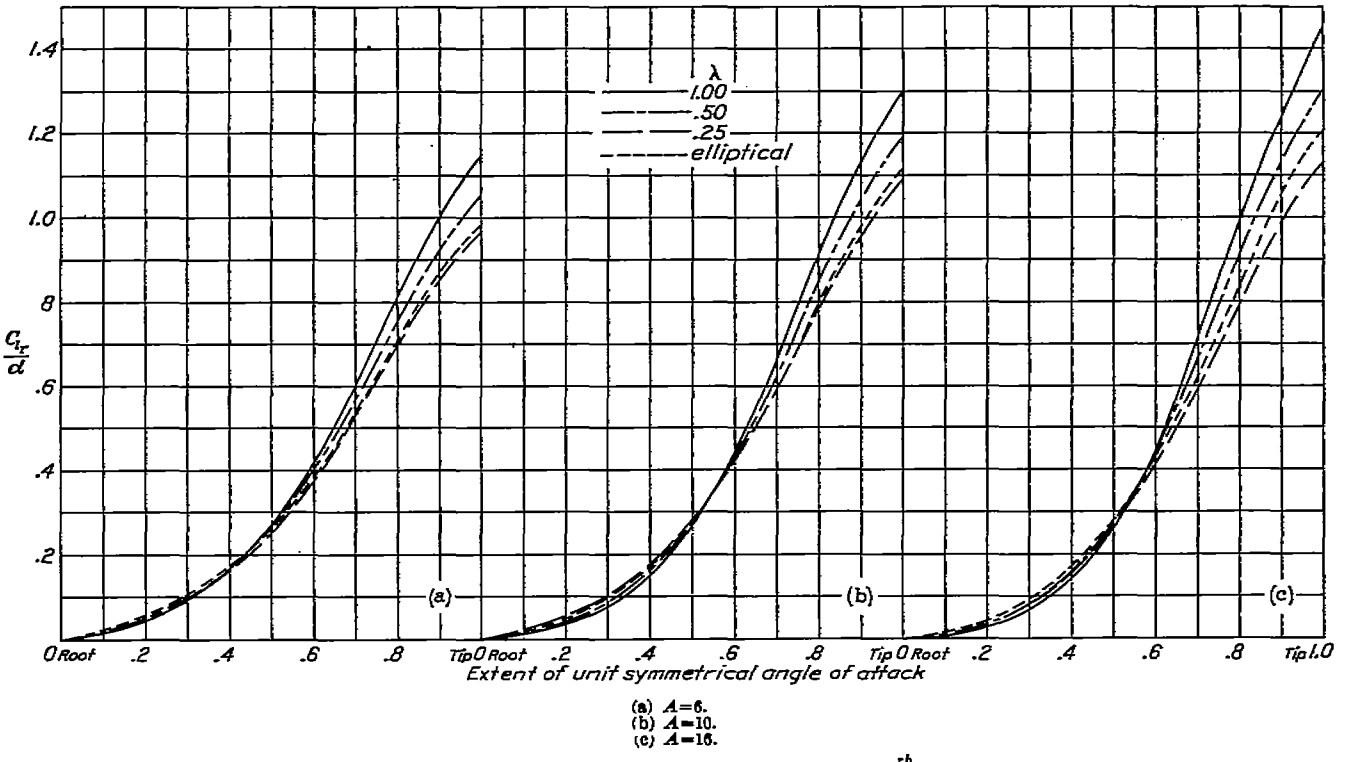


(a) $A=6$.
(b) $A=10$.
(c) $A=16$.

FIGURE 11.—Rolling derivative due to yawing. $L_{yawing}=C_{l_r}\frac{rb}{2V}qSb$

in contrast to the system given by equation (18) of reference 2.

By means of equation (9), Fourier coefficients were computed for the nine tapered wings with two different initial angle-of-attack distributions: (1) a distribution due to a unit angle of attack extending over the whole span, and (2) a unit angle of attack at the wing center covering half the span. In order to obtain the correct fairing of the final curves of figure 11, similar results were computed for elliptical wings with six angle-of-attack distributions covering 0, ¼, ½, ¾, ⅞, and all of the wing span.

As was the case with the derivative $C_{n_p}$, it is most convenient to give the derivative of rolling moment

due to yawing $C_{l_r}$ as a ratio in terms of a partial-span unit angle of attack. The values of $C_{l_r}$ may be obtained from figure 11 and are to be inserted into the equation

$$L_{yawing}=C_{l_r}\frac{rb}{2V}qSb \tag{10}$$

By the process described in the previous section, values of $C_{l_r}$ may be obtained for wings with any initial twist distribution that is symmetrical about the center line.

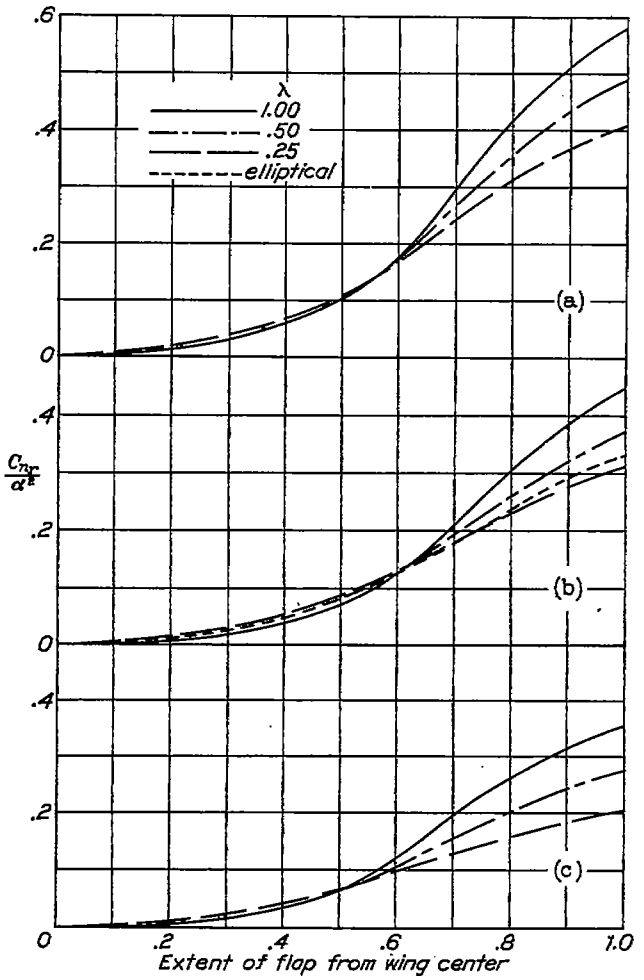


(a) $A=6$.
(b) $A=10$.
(c) $A=16$.

FIGURE 12.—Yawing derivative due to yawing for partial-span flap.

$N_{yawing}=C_{n_r}\frac{rb}{2V}qSb$

The curves of figure 11 fall in the order that would be expected for the various taper ratios, i. e., the moment for an untwisted tapered wing would be expected to be less than that for a rectangular wing of the same span and area because the tapered wings have a smaller proportion of the wing area at the tip. On account of the induced velocities along the span, the reduction, for the tapered wings, is not so great as would be obtained by an application of the ordinary strip theory.

The direction of the moment is such that, with the system of axes used, a positive rolling moment generally results from a positive yawing velocity when the wing is giving positive lift. By the use of considerable washout, such as is obtained with partial-span flaps, it is possible not only to reduce the value of this moment but also to make it slightly negative for low wing lift coefficients.

As was the case with $C_{l_p}$ and $C_{n_p}$, the value of $C_{l_r}$ for the entire airplane is due almost wholly to the wings because the side area of the airplane contributes relatively little moment as compared with the wings in curvilinear flight.

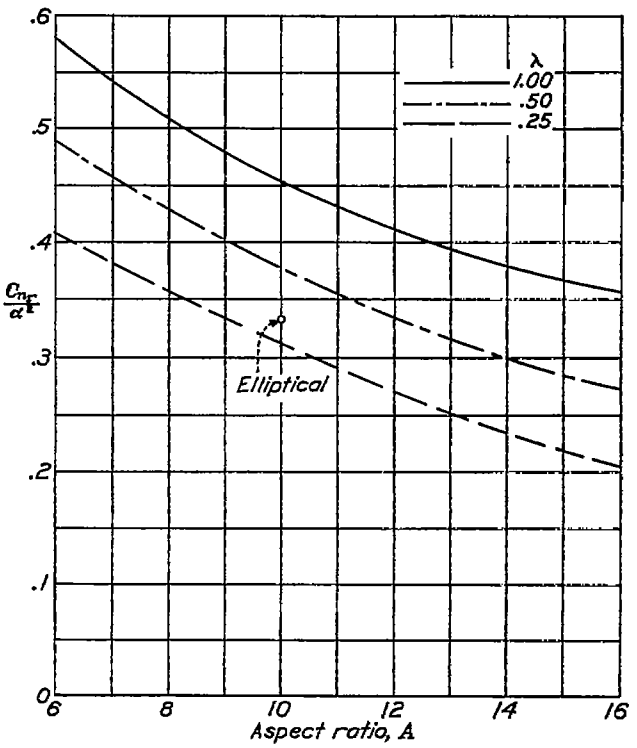


FIGURE 13.—Yawing derivative due to yawing for untwisted wing.

$N_{yawing}=C_{n_r}\frac{rb}{2V}qSb$

### YAWING MOMENT DUE TO YAWING

A part of the wing yawing moment due to yawing results from the change in the induced-drag distribution that accompanies the change in the lift distribution across the span of a yawing wing. The rest of the yawing moment is due to the difference in the distribution of profile drag resulting from the variation in velocity along the span. Both parts, however, produce damping moments in the unstalled-flight range.

The part of the wing yawing moment due to the induced drag is defined by the equation

$$N_{yawing}=C_{n_r}\frac{rb}{2V}qSb \tag{11}$$

where the derivative $C_{n_r}$ may be obtained from figure 12 for certain types of angle-of-attack distribution. The special distributions for which the derivatives of figure 12 apply are both uniform and symmetrical about the

wing center line. Such distributions occur only when partial-span flaps of constant-chord ratio are deflected, the rest of the span being at zero angle of attack. This limitation in the applicability of these curves as compared with the previous ones is due to the fact that the principle of superposition does not apply in cases where the variation is not linear with $\alpha$. The computed results may, however, be used to determine the variation of $C_{n_r}$ for the most useful case, namely, that of a wing without twist. For this purpose, the proper values of $C_{n_r}/\alpha^2$ obtained from figure 13, which is a cross plot of the end points of figure 12, are multiplied by the square of the actual angle of attack.

The part of the yawing moment due to the profile drag can be determined from the easily derived equation

$$\Delta N_{yawing}=q\int_{-\frac{b}{2}}^{\frac{b}{2}} c_{d_0}c\left(1+\frac{2ry}{V}\right)y\,dy \qquad (12)$$

where $c_{d_0}$ and $c$ are functions of the distance $y$ along the span. It is possible, by assuming $c_{d_0}$ constant and by neglecting terms of the second order, to obtain a coefficient $\Delta C_{n_r}$ that may be used with the equation

$$\Delta N_{yawing}=\Delta C_{n_r}\frac{rb}{2V}qSb \qquad (13)$$

to compute the part of the yawing moment due to the profile drag. The values of the profile yawing moment, as given by equation (13), are sufficiently accurate for most wings since $c_{d_0}$ generally varies only slightly across the span. The variation of the coefficient $\Delta C_{n_r}/C_{D_0}$ with taper ratio is given in figure 14.

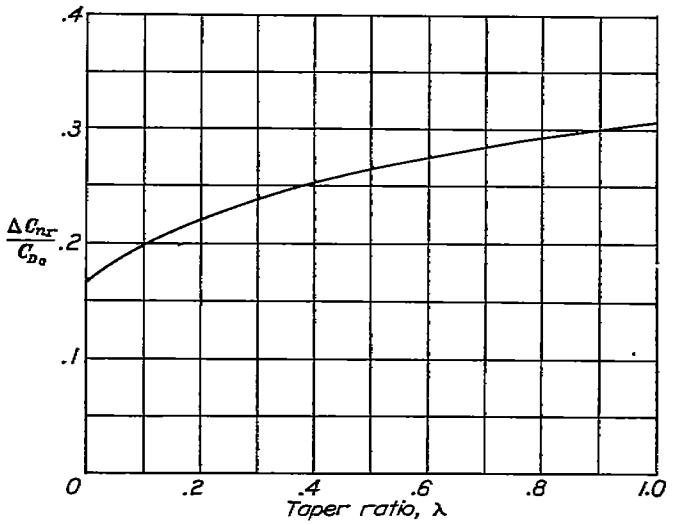


FIGURE 14.—Profile-drag yawing derivative. $\Delta N_{yawing}=\Delta C_{n_r}\frac{rb}{2V}qSb$

The total wing yawing moment due to yawing is the sum of the moments given by equations (11) and (13). At low lift coefficients, the profile drag contributes the greater portion of the wing damping moment in yawing. At moderate or high lift coefficients, however, the part due to the induced drag exceeds that due to the profile drag. If it is assumed that $\alpha=0.3$ and $C_{D_0}=0.01$, then the respective values of $C_{n_r}$ and $\Delta C_{n_r}$ would be 0.0522 and 0.0031 for a rectangular wing of aspect ratio 6.

The damping moment contributed by the wings in yawing motion is, in most cases, secondary but is not

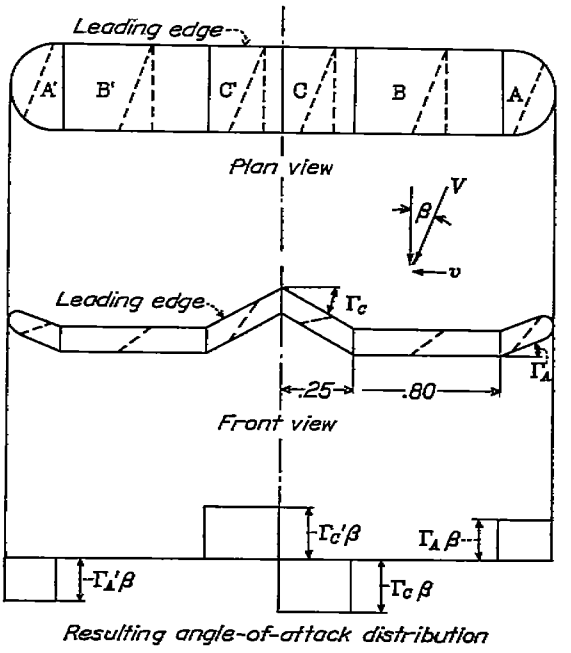


FIGURE 15.—Effect of irregular dihedral on sideslip.

negligible with respect to the damping moment contributed by the fuselage and the vertical tail surfaces. The damping in yawing due to the wings depends upon the angle of attack as well as upon the plan form; therefore the relative amounts contributed by the wings and tail surfaces may vary considerably.

Although it was not possible to give a general chart for determining the damping in yawing for symmetrically twisted wings as was done with the previous derivatives, it can nevertheless be said that the addition of load toward the tips, whether by washin or by an increase in taper ratio, would increase the wing damping moment due to a yawing angular velocity.

### ROLLING MOMENT DUE TO SIDESLIP

The manner in which the changes in angle of attack that cause a rolling moment are brought about during a sideslipping motion is shown in figure 15 by a sketch of a wing having positive, negative, and zero dihedral over various portions of the span. For simplicity, the wing is assumed to have no initial twist and the dihedral angles are assumed constant over each of the portions A, B, and C. For small angles of sideslip $\beta$, the increase in angle at tip A is, to a first approximation, equal to $\Gamma_A\beta$; whereas, at the opposite tip A′, there is an equal decrease of the angle of attack. The portions B—B′, having no dihedral, contribute no change in angle of attack when the wing is sideslipping. At the center,

however, owing to the negative angle of dihedral $\Gamma_C$, there is an effective decrease in angle of attack over part C equal to $\Gamma_C\beta$ and on C′ there is a similar increase in angle. Figure 15 shows the resulting effective angle-of-attack distribution for the particular shape of dihedral assumed.

The effect of this distribution is similar to that caused by two pairs of ailerons equally and oppositely deflected with the inner pair opposing the rolling action of those at the tip. Positive areas of dihedral on the advancing wing tend to add load onto that wing. For the system of axes chosen, all areas with positive dihedral produce a negative rolling moment with a positive angle of sideslip. This moment, like the rolling moment due to roll, is independent of the initial wing twist as long as no portion of the wing becomes stalled.

The rolling-moment derivative due to sideslip $C_{l_\beta}$ may be determined from figure 16, which gives the variation of $C_{l_\beta}/\Gamma$ for various unit antisymmetrical angle-of-attack distributions (i. e., symmetrical portions with constant dihedral) that extend out from the wing center and cover various relative amounts of the wing semispan. In the usual case, where the dihedral angle $\Gamma$ is constant along each semispan, the value of the rolling moment due to a sideslip angle $\beta$ can be obtained from the equation

$$L_{sideslip}=C_{l_\beta}\beta qSb \qquad (14)$$

where the appropriate values of $C_{l_\beta}/\Gamma$, obtained from figure 16 at the relative distance equal to 1.0, are multiplied by the dihedral angle in radians. In more unusual cases as, for example, where only the tips are turned up or where the wing is given a gull shape for any reason, it is still possible to determine a coefficient of rolling moment due to sideslip simply by adding the effects of the various parts in the way previously described. Thus, for the wing shown in figure 15, let $A=6$, $\lambda=1.0$, $\Gamma_A$ and $\Gamma_C=0.1$ radian and assume that it is desired to find the proper value of $C_{l_\beta}$ to use in equation (14). The part due to the tip portions A—A′ is $\Delta_1$ (from fig. 16 (a)) $\times$ $\Gamma_A=0.195\times 0.1=0.0195$. The part due to the center portions C—C′ is $\Delta_2\times\Gamma_C=0.065\times0.1=0.0065$. The resulting value of $C_{l_\beta}$ to be used in equation (14) is thus 0.0130. The extension of this method to a curvilinear variation of $\Gamma$ along the span may be easily made by plotting the values of $\Gamma$ at each point of the span and using the method given in a previous section for integrating for the total effect.

The results of figure 16 indicate that equivalent angle-of-attack changes caused by unit lengths of dihedral portion near six-tenths of the relative distance from the center are, in general, slightly more effective in producing rolling moment than unit lengths of dihedral at the tips. Such a result is due partly to the fact that the load curves near the tips are rounded and partly to the fact that, for the tapered wings, the larger areas affected by lengths of dihedral near the 0.6 point tend to compensate for the shorter moment arms through which the change in loading acts.

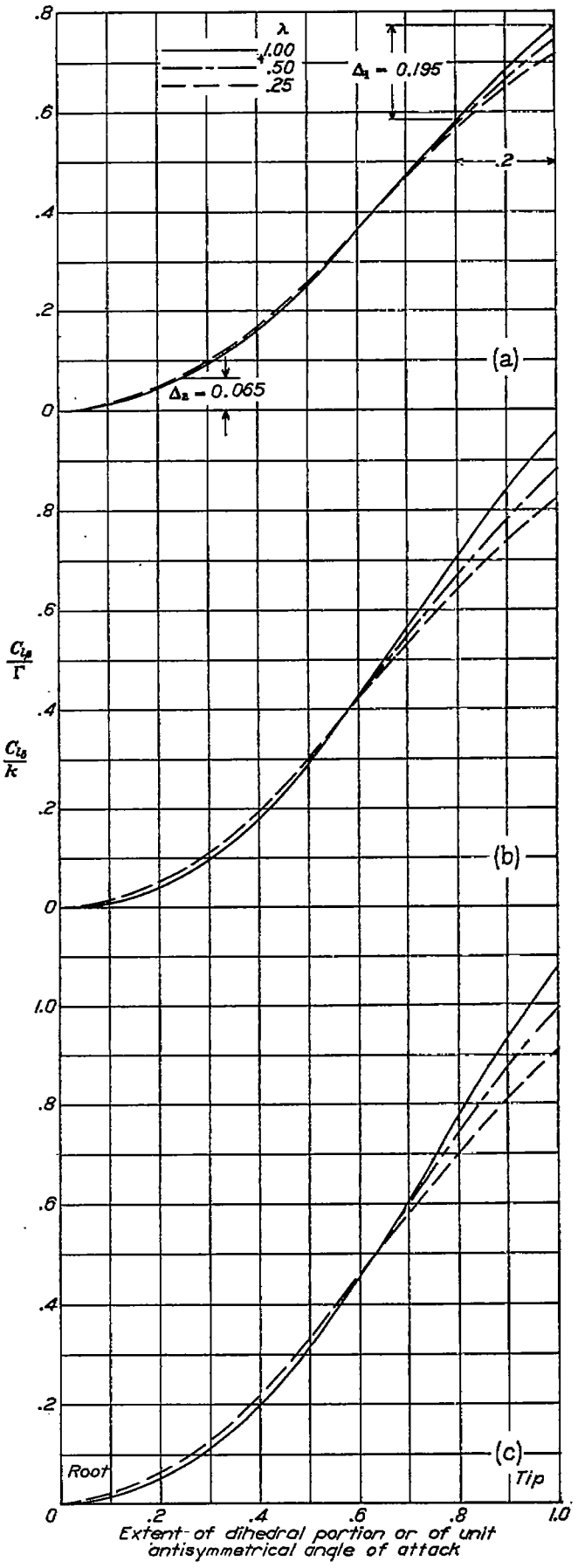


(a) $A=6$. (b) $A=10$. (c) $A=16$.

FIGURE 16.—Rolling derivative due to sideslip with dihedral. $L_{sideslip}=C_{l_\beta}qSb$

Although, during a sideslipping motion, positive dihedral produces a righting moment, a similar though generally smaller effect may also be produced by the addition of vertical area above the longitudinal wind axis. Also, on account of interference effects, the proportion of the airplane rolling moment contributed by the wings may vary considerably with the external appearance of the airplane.

It is usually considered, in practice, that a straight wing will have some dihedral effect, but tests of wings with well-rounded tips (reference 5) do not support this view. In cases of wings with blunt tips or in cases where chords of the sections near the tip do not lie in one plane, some dihedral action is shown.

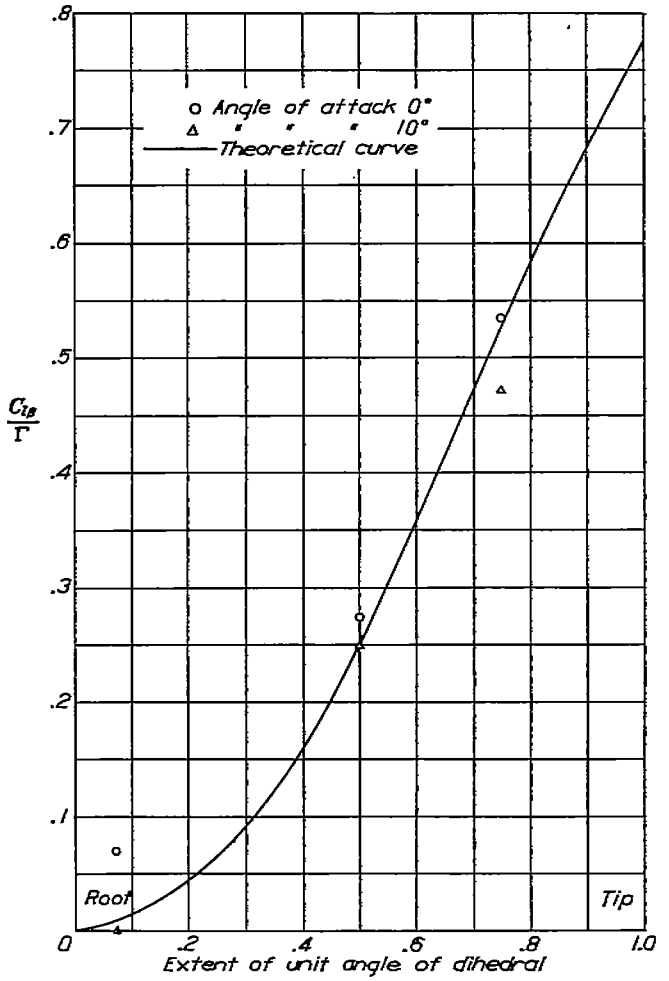


FIGURE 17.—Comparison between experimental and computed values of $C_{l_\beta}/\Gamma$ (experimental data from reference 5).

Figure 17 shows a comparison of experimental and computed values of $C_{l_\beta}/\Gamma$. The experimental values have been obtained from figure 23 of reference 5 and the coefficients given therein have been converted to the form used in this report. In the tests reported in reference 5, a rounded-tip rectangular wing of aspect ratio 6 was given various lengths of dihedral by turning up the outer portions of the wing. Each wing was then tested throughout the angle-of-attack range for various sideslip and dihedral angles.

It will have been apparent from the preceding discussion that the results of figure 16 may also be applied to predict the rolling moment caused by an aileron deflection in unyawed flight since ailerons, equally and oppositely deflected, cause changes in the angle-of-attack distribution that are similar to the changes caused by dihedral. Strictly speaking, however, the change in angle of attack due to dihedral cannot have quite the same effect as a similar change produced by ailerons because the ordinary lifting-line theory, when applied to yawed or sweptback wings, omits the effect of the stagger of the trailing vortices and the inclination of the bound vortex. Although the present theory has not been modified to take this effect into account, there

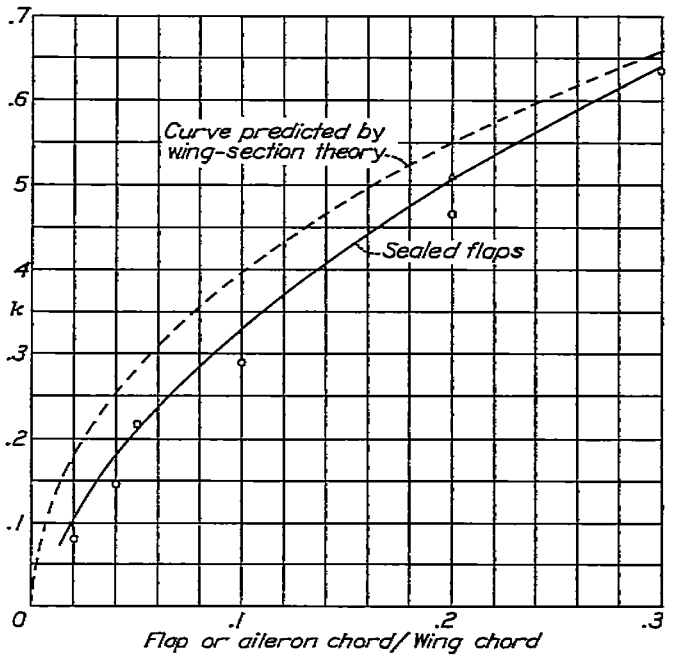


FIGURE 18.—Variation of $k$ with ratio of flap or aileron chord to wing chord.

is ample justification for omitting it in the computations as experiments indicate only second-order differences (see reference 5) for the usual angles of yaw and sweepback.

For the computation of the rolling moment due to an aileron deflection $\delta$, the appropriate value of $C_{l_\delta}$ to be inserted in the equation

$$L_{ailerons}=C_{l_\delta}\delta qSb \tag{15}$$

may also be found from figure 16. The derivative $C_{l_\delta}$ is given as a ratio in terms of $k$, the theoretical change of $\alpha$ with aileron deflection. Although the value of $k$ has been theoretically determined for thin wings, it is better to use values of $k$ determined from an analysis of experimental data. For this purpose, figure 18 is included, which shows the variation of $k$ for values of the ratio of aileron or flap chord to wing chord up to 0.3. This variation of $k$ has previously been given in figure 11 of reference 6 and holds for sealed flaps deflected up to approximately 20°.

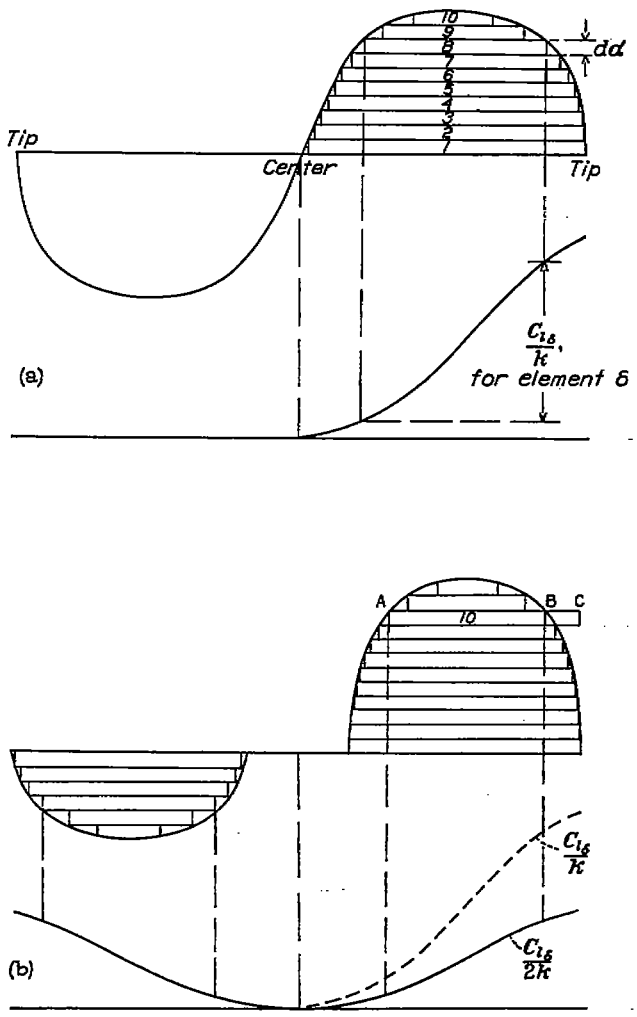


(a) Ailerons deflected equally.
(b) Ailerons deflected differentially.

FIGURE 19.—Addition of effect of aileron elements.

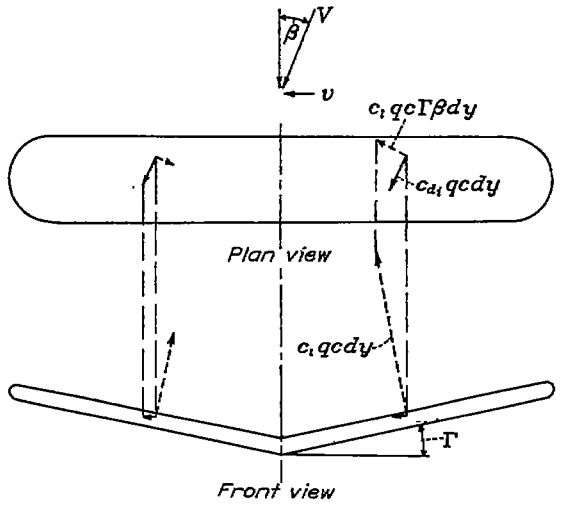


FIGURE 20.—Action of dihedral in producing yawing moment in sideslip.

If the angle-of-attack change caused by deflecting the ailerons is antisymmetrical about the wing center line, the proper value of $C_{l_\delta}$ to be used with equation (15) (for the rolling moment only) can be found by an integration or summation of the effects of elemental ailerons of various lengths and positions along the span as indicated in figure 19 (a). The values of $C_{l_\delta}/k$ are obtained from figure 16 for the wing plan form used. If the ailerons are differentially operated, then it may be better to divide the ordinates of figure 16 by 2 and to determine the value of the moment given by each aileron as indicated in figure 19 (b).

### YAWING MOMENT DUE TO SIDESLIP

The yawing moment of a wing with dihedral in sideslipping motion may be conveniently divided into two parts, the first part being due to the unsymmetrical

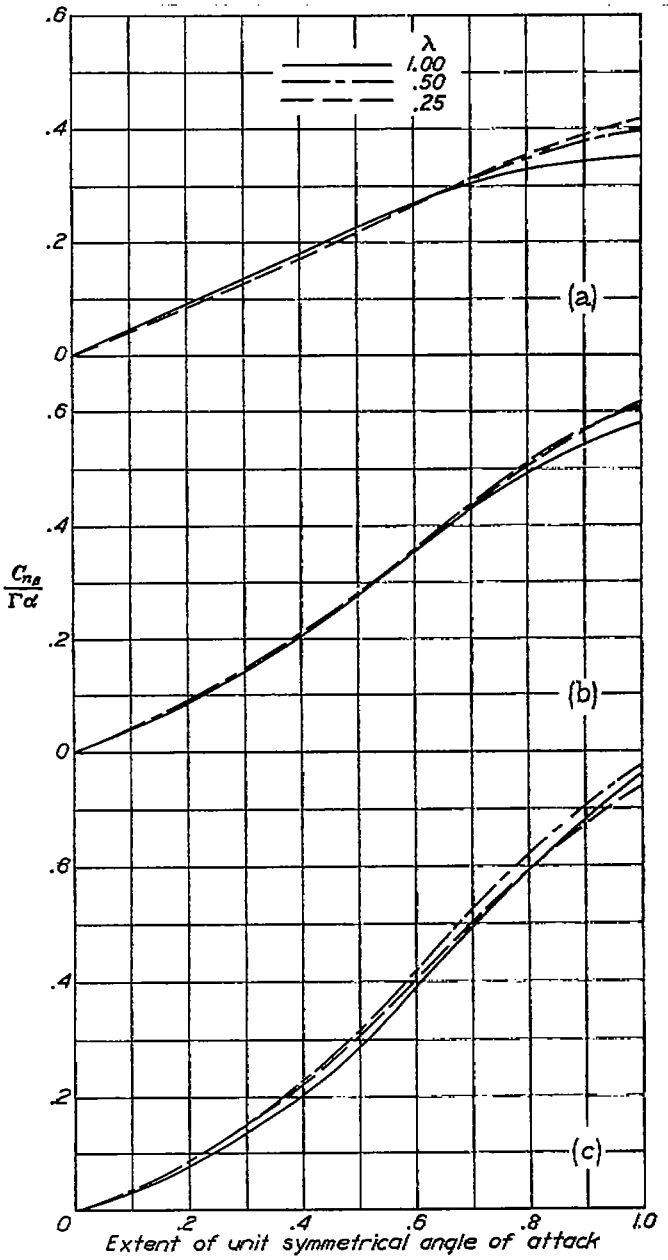


(a) $A=6$.
(b) $A=10$.
(c) $A=16$.

FIGURE 21.—Yawing derivative due to sideslip (dihedral constant).
$N_{sideslip}=C_{n_\beta}\beta qSb$

induced-drag distribution over the span and the second part due to a shift of the lift vectors acting so as to produce a moment about the vertical axis. Figure 20 illustrates the components of the section lift and drag vectors that produce yawing moments. The advanced wing having the larger lift will also have a larger induced drag and hence a component moment is set up that tends to turn the wing so as to reduce the sideslip; at the same time, however, the contrary moment due to the components of the lift acts to advance the forward half of the wing still more. As was the case with the yawing derivative due to rolling, the moments caused by the lift components predominate and, as a result, the net theoretical moment is an unstable one; or, in other words, with the system of axes chosen, a negative yawing moment results when the dihedral and sideslip angles are positive.

The explanations advanced in some textbooks neglect the inward slope of the lift vectors and lead to an incorrect sign of the yawing moment.

The yawing moment in sideslip is given by the equation

$$N_{sideslip}=C_{n_\beta}\beta qSb \tag{16}$$

The derivative $C_{n_\beta}$ is given in figure 21 as a ratio in terms of $\Gamma\alpha$ because its value depends linearly upon the magnitude of the product of these variables. The values of $C_{n_\beta}/\Gamma\alpha$ have been computed for unit symmetrical angle-of-attack distributions that extend out on either side of the center line and cover 0.25, 0.50, 0.75, and all of the wing span. These curves may be used to determine values of $C_{n_\beta}$ for any initial angle-of-attack distribution symmetrical about the wing center line, provided also that the angle of dihedral is constant across the wing span. Although the rolling derivative due to sideslip can be obtained (from fig. 16) for a curvilinear variation of dihedral along the span, it is necessary to stipulate that either $\alpha$ or $\Gamma$ remain constant if the principle of superposition is to be applied in the determination of $C_{n_\beta}$. The combination of variable symmetrical twist and uniform dihedral being more common than the converse, the computations were shortened by including curves for only the case of uniform dihedral.

The resultant value of $C_{n_\beta}$ (to be used in equation (16)) is found by either an integration or a summation of the effects of elements of angle of attack extending along the span. The process to be followed where graphical evaluation is necessary has been illustrated in figure 10, with the ordinates of figure 10 (a) changed to $\Gamma\alpha$. The ordinates and abscissas of the remaining parts are to be changed as required. For untwisted wings with uniform dihedral, the value of $C_{n_\beta}/\Gamma\alpha$ is obtained by multiplying the value read at a relative distance of 1.0 by the wing angle of attack and, in turn, by the dihedral angle.

The curves of figure 21 being generally steeper beyond the 0.5 point, the deduction of increments of angle of attack at the tip, i. e., giving the wing washout, would be the simplest means of decreasing the unstable yawing moment caused by the wings in a sideslipping motion.

Although the predicted variation of the yawing moment with dihedral is confirmed, experiments show a residual stable yawing moment at zero dihedral that is not predicted by the ordinary theory. This residual moment is greater for wings with blunt tips and is greater at zero or negative lifts. It will be noted that the theoretical yawing moment is itself the small resultant of two large contrary effects and is thus of the same order as a number of possible secondary influences.

LANGLEY MEMORIAL AERONAUTICAL LABORATORY,
NATIONAL ADVISORY COMMITTEE FOR AERONAUTICS,
LANGLEY FIELD, VA., *April 19, 1938.*

## REFERENCES

1. Lotz, Irmgard: Berechnung der Auftriebsverteilung beliebig geformter Flügel. Z. F. M., 22.Jahrg., 7.Heft, 14.April 1931, S. 189–195.
2. Pearson, H. A.: Span Load Distribution for Tapered Wings with Partial-Span Flaps. T. R. No. 585, N. A. C. A., 1937.
3. Betz, A., and Petersohn E.: Contribution to the Aileron Theory. T. M. No. 542, N. A. C. A., 1929.
4. Pearson, H. A.: Theoretical Span Loading and Moments of Tapered Wings Produced by Aileron Deflection. T. N. No. 589, N. A. C. A., 1937.
5. Shortal, Joseph A.: Effect of Tip Shape and Dihedral on Lateral-Stability Characteristics. T. R. No. 548, N. A. C. A., 1935.
6. Weick, Fred E., and Jones, Robert T.: Résumé and Analysis of N. A. C. A. Lateral Control Research. T. R. No. 605, N. A. C. A., 1937.

TABLE I.—VALUES OF COEFFICIENTS DEFINING WING CHORD DISTRIBUTION

$$\frac{c_x}{c}\sin\theta=\Sigma\, C_n\cos n\theta$$

$C_0$

| A \ λ | 1.00 | 0.50 | 0.25 | Elliptical |
|---|---|---|---|---|
| 6 | 0.730 | 1.000 | 1.300 | 1.000 |
| 10 | .700 | .956 | 1.270 | 1.000 |
| 16 | .677 | .932 | 1.240 | 1.000 |

$C_2$

| A \ λ | 1.00 | 0.50 | 0.25 | Elliptical |
|---|---|---|---|---|
| 6 | −0.260 | −0.149 | ---------- | ---------- |
| 10 | −.320 | −.218 | ---------- | ---------- |
| 16 | −.368 | −.259 | −0.121 | ---------- |

$C_4$

| A \ λ | 1.00 | 0.50 | 0.25 | Elliptical |
|---|---|---|---|---|
| 6 | ---------- | −0.074 | −0.207 | ---------- |
| 10 | ---------- | −.140 | −.220 | ---------- |
| 16 | −0.040 | −.154 | −.323 | ---------- |